AD_____

GRANT NUMBER DAMD17-96-1-6254

TITLE: Computer-Aided Diagnosis and Feature-Guided Data Reduction Systems in Mammography

PRINCIPAL INVESTIGATOR: Heang-Ping Chan, Ph.D.

CONTRACTING ORGANIZATION: University of Michigan
Ann Arbor, MI 48103-1274

REPORT DATE: October 1997

TYPE OF REPORT: Annual

PREPARED FOR: Commander
U.S. Army Medical Research and Materiel Command
Fort Detrick, Frederick, Maryland 21702-5012

REPORT DOCUMENTATION PAGE

Form Approved
OMB No. 0704-0188

1. AGENCY USE ONLY *(Leave blank)*	2. REPORT DATE	3. REPORT TYPE AND DATES COVERED
	October 1997	Annual (23 Sep 96 - 22 Sep 97)

4. TITLE AND SUBTITLE
Computer-Aided Diagnosis and Feature-Guided Data Reduction Systems in Mammography

5. FUNDING NUMBERS
DAMD17-96-1-6254

6. AUTHOR(S)
Heang-Ping Chan, Ph.D.

7. PERFORMING ORGANIZATION NAME(S) AND ADDRESS(ES)
University of Michigan
Ann Arbor, MI 48103-1274

8. PERFORMING ORGANIZATION REPORT NUMBER

9. SPONSORING/MONITORING AGENCY NAME(S) AND ADDRESS(ES)
Commander
U.S. Army Medical Research and Materiel Command
Fort Detrick, Frederick, Maryland 21702-5012

10. SPONSORING/MONITORING AGENCY REPORT NUMBER

11. SUPPLEMENTARY NOTES

12a. DISTRIBUTION / AVAILABILITY STATEMENT
Approved for public release; distribution unlimited

12b. DISTRIBUTION CODE

13. ABSTRACT *(Maximum 200*

The goals of this project are: (1) Implement and evaluate a computer-aided diagnosis (CAD) system to assist radiologists in mammographic interpretation. (2) Develop and evaluate a feature-guided data compression technique to facilitate implementation of digital mammography.

For the first sub-project, we plan to implement our CAD algorithms for detection and classification of microcalcifications in a high speed workstation, develop user interface for efficient operation of the CAD programs, and perform a pilot clinical trial in three mammographic screening sites. For the second sub-project, we plan to evaluate different data compression techniques. We will select the most efficient lossless technique and the lossy technique that can provide maximum compression ratio without noticeable loss of information for mammography.

In the first year of the funding period, we have performed the following studies: (1) development of a graphical user interface (GUI) for the CAD, (2) conversion of CAD software from VMS to UNIX operating system, (3) improvement in the automated algorithms for detection of masses and microcalcifications, (4) study of data compression methods for mammograms, and (5) design methods for data collection and data analysis for the pilot clinical trial. These studies are the necessary steps to accomplish the goals of this project.

14. SUBJECT TERMS Breast Cancer Mammography
Computer-aided diagnosis, data compression, breast cancer detection

15. NUMBER OF PAGES
21

16. PRICE CODE

17. SECURITY CLASSIFICATION OF REPORT	18. SECURITY CLASSIFICATION OF THIS PAGE	19. SECURITY CLASSIFICATION OF ABSTRACT	20. LIMITATION OF ABSTRACT
Unclassified	Unclassified	Unclassified	Unlimited

FOREWORD

Opinions, interpretations, conclusions and recommendations are those of the author and are not necessarily endorsed by the U.S. Army.

____ Where copyrighted material is quoted, permission has been obtained to use such material.

____ Where material from documents designated for limited distribution is quoted, permission has been obtained to use the material.

____ Citations of commercial organizations and trade names in this report do not constitute an official Department of Army endorsement or approval of the products or services of these organizations.

____ In conducting research using animals, the investigator(s) adhered to the "Guide for the Care and Use of Laboratory Animals," prepared by the Committee on Care and Use of Laboratory Animals of the Institute of Laboratory Resources, National Research Council (NIH Publication No. 86-23, Revised 1985).

NPC _X_ For the protection of human subjects, the investigator(s) adhered to policies of applicable Federal Law 45 CFR 46.

____ In conducting research utilizing recombinant DNA technology, the investigator(s) adhered to current guidelines promulgated by the National Institutes of Health.

____ In the conduct of research utilizing recombinant DNA, the investigator(s) adhered to the NIH Guidelines for Research Involving Recombinant DNA Molecules.

____ In the conduct of research involving hazardous organisms, the investigator(s) adhered to the CDC-NIH Guide for Biosafety in Microbiological and Biomedical Laboratories.

Chan Heang Ping 10/20/97

PI - Signature Date

(4) Table of Contents

(5) Introduction

In the United States, breast cancer is the leading cause of death in women between 40 to 55 years of age[1]. It is estimated that one out of eight women will develop breast cancer in their lifetime [2, 3]. There is considerable evidence that early diagnosis and treatment significantly improves the chance of survival for patients with breast cancer [4-9]. The American Cancer Society — National Cancer Institute Breast Cancer Detection Demonstration Project (BCDDP) has shown that mammography contributes significantly in the detection of localized breast cancer in asymptomatic women [9].

Although mammography has a high sensitivity for detection of breast cancers when compared to other diagnostic modalities, studies indicate that radiologists do not detect all carcinomas that are visible on retrospective analyses of the images [8, 10-18]. While double reading can reduce the miss rate in radiographic reading [19, 20], it also increases the cost of screening. In our ROC study [21], we found that a CAD scheme, which alerts the radiologist to suspicious clusters of microcalcifications, can significantly improve radiologists' accuracy in detecting the microcalcifications under experimental conditions that simulate the rapid interpretation of screening mammograms. More recently, Kegelmeyer et al. [22] also showed that CAD can improve radiologists' detection of spiculated masses. These studies indicate that CAD is a viable alternative to double reading by radiologists.

Early breast cancers are often characterized by subtle clustered microcalcifications and masses [23]. It has been reported that between 30 and 50% of breast carcinomas detected radiographically demonstrate microcalcifications on mammograms, and 40 to 50% of breast carcinomas present as masses. The high correlation between the presence of microcalcifications and masses and the presence of breast cancers indicates that an increase in the accuracy of detection and analysis of the characteristic features of these lesions may lead to further improvement in the efficacy of mammography as a screening procedure for the detection of early breast cancer.

In the past few years, we have been developing CAD algorithms in detection and classification of microcalcifications and masses using advanced image processing and computer vision techniques. Our CAD algorithms have provided very promising results in laboratory tests. At this stage, it is necessary to test the algorithms in a clinical trial with a large number of mammograms obtained from the general patient population before specific methods can be developed to further improve their performance. Therefore, our goals in this proposal are to implement our CAD algorithms in a fast workstation, develop user interfaces for efficient operation of the CAD programs, and conduct a pilot clinical trial of the CAD schemes at three mammographic screening sites. Based on the results of the pilot clinical trial, we can evaluate the sensitivity and specificity of the CAD algorithms, analyze the effects of the CAD schemes on mammographic screening, identify any potential problems in a clinical environment, and develop methods to further improve the CAD schemes in the future. We believe that this is a crucial step to develop a clinically practical CAD workstation.

It has been recognized that digital mammography is one of the key research areas for improvement in the diagnosis of breast cancer [24]. Two of the major issues in digital mammography are the technological requirements in developing high resolution digital detectors and the transmission and archiving the large amount of data. A number of solid-state large-area digital detectors are being developed for mammographic application. It has been generally recognized that a pixel size of no greater than 0.05 mm $\times$ 0.05 mm will be required for imaging the subtle features of microcalcifications. At this resolution, a single 8" $\times$ 10" mammogram will result in 40 MB of digital data.

Data compression can reduce the amount of data for transmission and storage. However, there is often a tradeoff between compression ratio and image fidelity. Data compression in mammography is

especially difficult because of the very subtle image details such as microcalcifications and mass margins that need to be preserved. We have investigated the effects of data compression on computerized detection of microcalcifications previously. In the current proposal, we plan to develop a CAD guided data compression technique to maximize the compression efficiency with a minimum loss of information. Our approach is to preserve the original image information by lossless compression in potentially important regions on the mammograms indicated by the CAD programs. For breast areas outside these regions, we will apply the most efficient lossy compression technique that does not cause noticeable degradation of image details. We will conduct both receiver operating characteristic studies and subjective image quality ranking studies to compare observer performance on the uncompressed images, on images compressed with the selected lossy technique, and on images compressed with the standard JPEG technique.

The importance of this research is based on the fact that x-ray mammography is, at present, the most reliable diagnostic procedure for detection of early breast cancer. Our proposed research aims at the development of a CAD workstation which may assist radiologists in screening and characterizing abnormalities on mammograms and the development of an efficient CAD-guided data compression technique for digital mammography. The CAD workstation, once developed, can be implemented and operated cost-effectively in various breast imaging facilities as a second opinion, and thus will potentially increase the diagnostic accuracy of mammography for breast cancer detection. The data compression technique will facilitate the implementation of telemammography and digital mammography for breast cancer screening. These new technologies therefore are expected to have a significant impact on patient care, especially in rural and remote areas.

(6) Body

During the funding period of 9/22/96 to 9/21/97, the three collaborating institutions, University of Michigan, Georgetown University, and University of Iowa, have conducted the following tasks:

(a) Development of a graphical user interface (GUI) for the CAD workstation

One of the aims of this project is to develop a GUI for implementation of the CAD software in a workstation. We have designed a GUI based on the need and requirements for our project. The application should be as independent of operating systems as possible, present a comfortable and customizable user interface, and provide the developer with a reasonably simple means of incorporating new analysis tools. By employing a modified architecture based upon the Model-View-Controller scheme developed in the Smalltalk environment, it is hoped that these goals can be met. This architecture provides a means to separate the window-system dependent operations of displaying data and receiving user commands from the data manipulation code. To this end, it seems that an object-oriented approach using C++ to structure programs using the Xt/Motif graphical interface will be reasonable. There are hundreds of user interface toolkits available that support a variety of languages and programming styles. However, issues such as future availability, acceptance by users and programmers, support, and reliability have affected this choice. We have found, via the World Wide Web, a software (developed by Douglas Young) which provides a framework that facilitates the GUI development. Creation of X widgets, button interfaces and their callback registration, incorporation of the users' application defaults specifications (colors, fonts, etc), and so forth have been encapsulated in a number of reliable and reusable C++ classes so that the programmer can focus more on the application behavior and less on the user interface implementation details.

The current status of the program is described here. A main window is presented which includes a menubar, a scrolled display area, and a system command interface. The menubar supports hierarchical menus. Menu choices are added simply by providing command procedures and adding them to a list. The framework creates the necessary buttons, registers the appropriate callback mechanism, and manages or unmanages the widgets. There is a facility to selectively enable or disable menu choices as appropriate to the current state of the application. The display area uses a grayscale colormap to present images. It will change size in response to the user resizing the main window, present appropriate portions of the image in response to changes in scrollbar positions, and refresh the image when an obscured portion is uncovered. The command interface allows the user to issue commands to the operating system from within the application, and presents a history list of previous commands that can be selected for reissuance.

The main menu choices will contain many functions, including File, Edit, View, Process, Tools, Window, and Help. Many image manipulation functions will be developed under each menu. For example, under the 'File' choice are the following. There is a single level 'undo' that is active when a command provides this functionality. It is automatically made available or unavailable as appropriate. The 'open' choice presents a pop-up file selection dialog that permits browsing through filesystems and the selection of files. The 'new' command creates another main window capable of displaying a different image with its own colormap. Currently, the only colormap available is the grayscale, however, a facility allowing a user created or specified map will be included. The 'close' command destroys its main window, unless it is the last one. The 'submenu' choice demonstrates the hierarchical menu facility by presenting a submenu with a few of the above choices included to prove functionality. The 'quit' choice simply exits the application, destroying all of its windows, after user affirmation of intent. Under the 'Help' menu there is the 'Version' command, which reports the revision number of the

program. Under the 'view' menu, there will be windowing, zooming, panning, and other image enhancement tools. Under the 'Process' menu, there will be all the CAD software and image processing functions. Under the 'Tool' menu, there will be region of interest (ROI) selection and manipulation, text and graphical overlay, etc.

Some commands, such a 'Quit' and 'New' are global in scope: no matter how many main windows are open or which one is currently active, they do the same thing. Others, such as 'Open' and 'Close', are local to the active main window. It is possible to link some local operations to operations in other main windows, since the application framework maintains lists of the appropriate X windows data. This has been temporarily demonstrated for the case of scrolling operations - - navigation within an image in one window can be propagated to all other active windows. It remains to be defined when this facility would be useful.

Presently, only one image format can be read. In progress is the definition of a C++ image class to contain the image data and the development of functions to read and write various image file formats, including DICOM. This class, or perhaps one derived from it, will include functions to perform various manipulations of the data, such as thresholding, windowing, histograms, filtering, region of interest designation, etc. Of particular concern is the amount of data presented by mammograms relative to available system memory. Several file and memory management methods are being examined with regard to efficiency and speed. Promising are several objects found in the Standard Template Library (STL) supplied with C++.

One highly desirable addition to the application framework will be an object that supports a user-customizable detachable toolbar that provides rapid access to frequently used operations. Another will be an extensive, context sensitive, help utility. Another will be a simple password verification method capable of restricting availability of certain procedures depending on the user's status (user vs developer) and preference file.

We will continue to develop the GUI for the CAD workstation. At the same time, the CAD programs for detection of masses and microcalcifications are being improved. These programs will be integrated into the CAD workstation via the GUI in the near future.

(b) Conversion of CAD software from VMS to UNIX operating system

Up to last year, our program development was based on the VMS operating system from the Digital Equipment Corporation (DEC). Because UNIX operating system is more commonly used in workstations and it allows more flexibility in selecting new workstations, peripherals, and software for future applications, we decided to migrate to UNIX early this year. We have to convert all of our CAD programs to run under UNIX. Many of the programs have to be modified and tested because there are some differences in the FORTRAN and C compilers under the two operating systems. Most of the modifications are relatively minor. However, some of the FORTRAN programs need major changes because the original versions incorporated subroutine utilities that are specific to DEC VMS operating systems. To-date, the conversion of the mass detection programs have been completed. The conversion of the microcalcification detection programs are near completion. These programs will be implemented in the CAD workstation and will be run with the GUI for the pilot clinical trial.

(c) Automated microcalcification detection program

We have been modifying the FORTRAN codes to make the programs portable between different operating systems, as described above. The programs will be interfaced to the GUI and it can be executed on a given input digitized mammogram via menu on the GUI. It can also be set up so that a group of digitized mammograms can be processed consecutively in batch mode overnight. The automated microcalcification detection program is one of the main components of the CAD workstation for the pilot clinical trial.

(d) Automated mass detection program

The mass detection scheme is now running under both VMS and UNIX. We can either apply the detection scheme in training or test mode. Training mode allows the classifiers at each stage of the algorithm to be trained while test mode allows a single image using a fixed classifiers and fixed thresholds to be run through the entire detection scheme. The test mode can also be set up to process a set of digitized mammograms in a batch mode. The mass detection code takes approximately 7 minutes per image using the current implementation and is currently able to detect 90% of the biopsy proven masses with 3.4 false-positives (FPs) per image or 80% of the masses with 1.4 FPs per image based on 255 test images containing a single biopsy proven mass. The mass detection is currently implemented using density-weighted contrast enhancement (DWCE) detection in the first stage and then refining the mass borders using gray-scale and gradient based region growing. Between each stage of the algorithm, morphological FP reduction using individual feature thesholding followed by linear discriminant classification is used. In the final step of the algorithm, texture features for each of the detected objects are calculated and used in a linear classifier to further differentiate between breast masses and normal structures.

We are currently investigate the use of fuzzy classifiers to improve both the morphological and feature classification. In addition, new morphological feature are under investigation to further differentiate normal structures from breast masses. We are in the process of testing the current detection scheme to an unknown image set. This independent test set will be used to gauge the robustness of our current implementation.

Accurate delineation of mass boundaries is an important step for the differentiation of true- and false-positives in an automated mass detection program. We evaluated both qualitatively and quantitatively the accuracy of two automated techniques for the segmentation of mass boundaries from regions of interest (ROIs). One hundred and fifteen mammograms with biopsy-proven masses were acquired from 58 patient files. The mammograms were digitized at 100 micron resolution. For each image, a fixed size ROI containing a mass was extracted. Two automated segmentation algorithms, one based on an adaptive clustering method using the gray level, edge gradient, and median-filtered images of the ROI and another based on statistical modeling of the ROI as a Gauss-Markov random field (GMRF), were used to extract mass boundaries. These boundaries were compared with manually segmented boundaries for 41 masses. Two quantitative measures, the mass fraction ratio index (MFRI) (the ratio of the intersection between the computer-segmented mass area and the manually segmented mass area to the computer-segmented mass area) and the percentage difference in the average radial length, extracted from the segmented mass were compared. A qualitative evaluation of 83 masses was also performed in which 5 observers rated the similarity of the two computer-segmented mass boundaries to the perceived mass boundary on a 10-point scale. The MFRI value for the algorithm based on the clustering was 0.95 and for that based on the GMRF model was 0.92. The mean differences in the average radial length feature were 13 and 20, respectively. The qualitative observer study indicated that the GMRF algorithm was marginally (2.5%) better than the clustering algorithm. Our quantitative and qualitative evaluation indicates that the segmented masses obtained from the

automated algorithms are reasonably close to those from manual segmentation. Morphological feature values obtained from automated and manual segmentations were comparable.

These techniques improve the mass segmentation from the current technique used in our mass detection programs that are based on thresholding and edge detection. We will incorporate the new segmentation techniques into our mass detection programs. The morphological features derived from the masses segmented with the improved method are expected to be more effective for reducing false-positives.

(e) CAD-guided data compression

We are developing data compression method for compressing digitized mammograms. Because of the high spatial resolution and high image fidelity required for mammograms, image compression methods specifically tailored to mammographic images are needed. The researchers in the Georgetown University have been investigating new image compression methods for mammograms. The following summaries their progresses.

1. Dyadic Data Decomposition

1.1 A Unification System

A decomposition method (H+GP) generalized from Haar transform has been derived. This general form can exactly describe dyadic doublet-type transforms such as orthogonal wavelets. Another general form (B+GP) based on the binomial filter can describe dyadic triplet-type transforms such as biorthogonal wavelets. Although the doublets and triplets seem to function independently, they share exactly the same decomposition principles. We can integrate major dyadic decomposition methods through a unified view. Figure 1 shows the unified perspective of dyadic decomposition systems we discover.

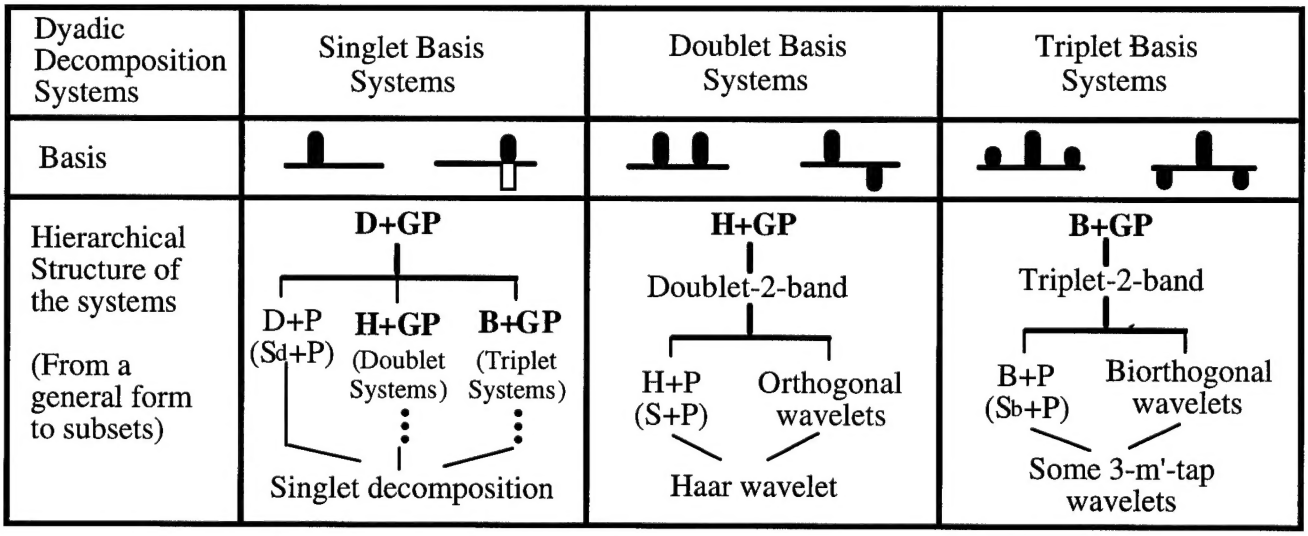

Figure 1. A diagram illustrates the unification of major dyadic decomposition systems.

The doublet- and triplet-types of dyadic transformation systems can be unified by the delta function basis (D+GP) decomposition system as following:

D+GP(delta+generalized prediction)

lowpass: $\hat{l}''_n = x_{2n} + a''(x_{2n\pm i})$ (1)

and

highpass: $\hat{t}''_n = x_{2n+1} + e''(x_{2n+1\pm i})$ (2)

where a" and e" are the added process and prediction terms, respectively. The well-known DPCM is a special case of the D+GP transform by giving $a''(.) = -x_{2n-1}$ and $e''(.) = -x_{2n}$. The doublet and triple decomposition systems are:

	H+GP(Haar+generalized prediction)	B+GP(binormal+generalized prediction)	
lowpass:	$\hat{l}_n = (x_{2n+1} + x_{2n})/2 + a(x_{2n\pm i})$	$\hat{l}'_n = (x_{2n-1} + 2x_{2n} + x_{2n+1})/4 + a'(x_{2n\pm i})$	(3)
and			
highpass:	$\hat{t}_n = (x_{2n+1} - x_{2n}) + e(x_{2n\pm i})$	$\hat{t}'_n = (2x_{2n} - x_{2n-1} - x_{2n+1}) + e'(x_{2n\pm i})$	(4)

1.2 Integer Implemenation of Wavelet transform

Based on the above theoretical development, we found that the general form can be used as a bridge for various dyadic decompositions. We are also successfully link the integer-based S transform and wavelet transform. A brief theory is given below:

For a set of digital data (i.e., an integer data sequence), Haar transform [25] can be approximated by Sequential (S) transform [26]. Basically, S transform computes the average and the difference of the two adjacent elements of the integer data sequence. More specifically, the former is the truncated integer of the average value. For a given data sequence X: $(x_i,\ i = 0,..N-1)$, the integer form of Haar transform (i.e., S transform) can be written as:

$$b_n = \lfloor (x_{2n} + x_{2n+1})/2 \rfloor \quad (5)$$

and $$d_n = x_{2n+1} - x_{2n}, \quad (6)$$

where $\lfloor . \rfloor$ stands for a truncation operation of a value. The corresponding inverse operations are:

$$x_{2n+1} = b_n + \lfloor (d_n + 1)/2 \rfloor \quad (7)$$

and $$x_{2n} = x_{2n+1} - d_n. \quad (8)$$

To further reduce the first-order entropy of the data sequence, we may add a prediction term, e_n, in the high pass domain for Eq. (2).

$$\hat{d}_n = (x_{2n+1} - x_{2n}) + \lfloor e_n + 1/2 \rfloor = d_n + \lfloor e_n + 1/2 \rfloor. \quad (9)$$

The addition of 1/2 and the truncation operation serves for integer implementation, otherwise they can be neglected. If the predictive values are statistically close to the values of $-d_n$, the reduction of the first-order entropy is achieved. The wavelet decomposition follows the similar concept of data prediction to reduce the entropy of the data sequence. In fact, we can use the adjacent decomposed Haar coefficients (i.e., b_n and d_n) to form an orthogonal wavelet transform through a prediction indicated in Eq. (9). First, let the prediction term be linearly composed by the adjacent decomposed coefficients, such that

$$e_n = \sum_i \alpha_i b_{n+i} + \sum_j \beta_j d_{n+j} \tag{10}$$

where α_i and β_j are the contribution factors of the decomposed Haar coefficients accordingly. Secondly, substitute Eq. (10) into (9) and let Eq. (9) equal to a scaled wavelet transform with a high pass convolution kernel $(\ldots -h_3, h_2, -h_1, h_0)$. By omitting the convolution operations with the data vector $\vec{x}$ for the both sides of the equation, we have

$$\begin{aligned}
&(\ldots\ldots\ldots\ldots\ldots)\times\alpha_i \\
&+(\ldots\ \tfrac{1}{2},\ \tfrac{1}{2},\ 0,\ 0)\times\alpha_{-1} \\
&+(\ldots\ 0,\ 0,\ \tfrac{1}{2},\ \tfrac{1}{2})\times\alpha_0 \\
&+(\ldots\ldots\ldots\ldots\ldots)\times\beta_j \\
&+(\ldots -1,\ 1,\ 0,\ 0)\times\beta_{-1} \\
&+(\ldots\ 0,\ 0, -1,\ 1)\times\beta_0 \\
&=\overline{(\ldots -h_3, h_2, -h_1, h_0)\times C}
\end{aligned} \tag{11}$$

where $b_n = (\ldots\ 0,\ 0,\ \frac{1}{2},\ \frac{1}{2})\otimes\vec{x}$, $b_{n-1} = (\ldots\ \frac{1}{2},\ \frac{1}{2},\ 0,\ 0)\otimes\vec{x}$, $d_n = (\ldots\ 0,\ 0, -1,\ 1)\otimes\vec{x}$, $d_{n-1} = (\ldots -1,\ 1,\ 0,\ 0)\otimes\vec{x}$, and so on. In addition, C is the offset scaled factor between the two transform systems and β_0 should be unity because the last term of the top form represents d_n.. The rest of the contribution factors (i.e., α_i and β_j) as well as C value can be solved in terms of the filter coefficients (i.e., h_i) of an m-tap transformation. Specifically:

$$\begin{aligned}
&C = 2/(h_0 + h_1). \\
&\alpha_0 = 2(h_0 - h_1)/(h_0 + h_1) \text{ and } \beta_0 = 1, \\
&\alpha_i = 2(h_{2i} - h_{2i+1})/(h_0 + h_1) \text{ and } \beta_j = (h_{2j} + h_{2j+1})/(h_0 + h_1).
\end{aligned} \tag{12}$$

A similar derivation can be extended to any 2-band filtering system. Based on Eq. (12), the decomposition coefficient is exactly the same as the high frequency coefficient through 2-band transform multiplied by the constant C. From Eq. (12), we can easily find that $\sum_i \alpha_i = C\sum_i (-)^i h_i$. Since the property of zero-mean filtering is maintained (i.e., $\sum_i (-)^i h_i = 0$) in an orthogonal wavelet or a 2-band filtering system, $\sum_i \alpha_i$ must vanish to match the case [27]. The above derivation indicates any orthogonal wavelet transform can be made by Haar Transform through prediction. In addition, the integer implementation, such that shown in Eq. (9), can be made by (i) downward truncation and (ii) use of approximated rational values of α_i and β_j. Since Eq. (9) can always be reversible, the accuracy of α_i and β_j values is not a concern as long as they are used consistently in both forward and inverse transforms.

For biorthnormal wavelets, the binomial decomposition would be the basis [28] and will also be studied. The transformed coefficients will then be encoded by embedded-zero-tree (EZW) [29] or

partitioning in hierarchical trees (PHT) [30]. Our recent studies indicated that both coding methods result in similar compression ratios. However, PHT seems to be computationally efficient.

1.3 Preliminary Study of the Wavelet Transforms using Real and Integer Value Computation

We have done several preliminary studies to prove that our algorithms are practical. Five CT and five mammograms were used to perform the forward and inverse transforms using regular dyadic wavelet decomposition as well as the integer implementation described above. Our study indicated that all images were fully reconstructed with two-dimensional transformation. Figure 2 shows an original CT profile. (Note profiles of mammogram are realtive shallow and are difficult to show the small differences in decomposed data). The decomposed profile based on regular wavelet transform (1-D) is shown in Figure 3. Its counterpart based on the integer version of the wavelet transform is shown in Figure 4. The low pass coefficients are almost the same. The main difference between the two decomposed high pass profiles appears at the sharp edge areas. This is because large values accentuate the computational differences between real and integer calculation. In fact, more number of small coefficients are found in the integer version of the profile. The first order entropy is 6.9 in the high pass profile using real computation. The first order entropy is 5.7 in the high pass profile in Figure 4. The excessive entropy results from the differences between the original and quantized profiles computed through real values. The quantization procedure is necessary for any real values to be encoded in a compression scheme.

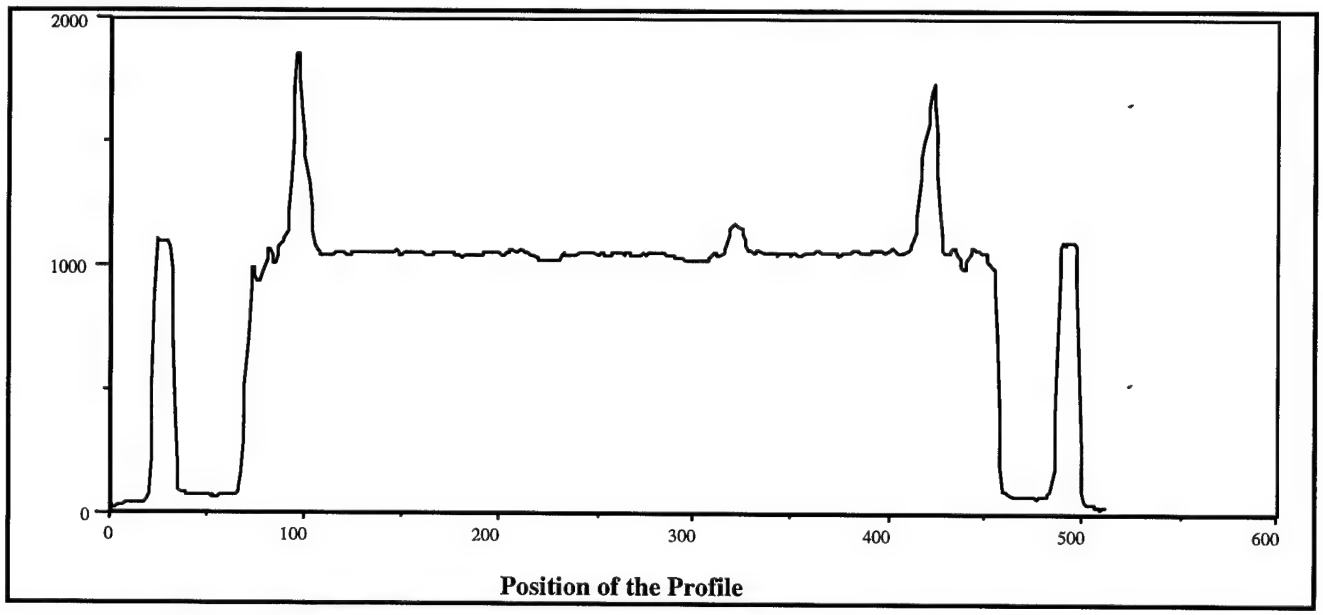

Figure 2. An original CT profile.

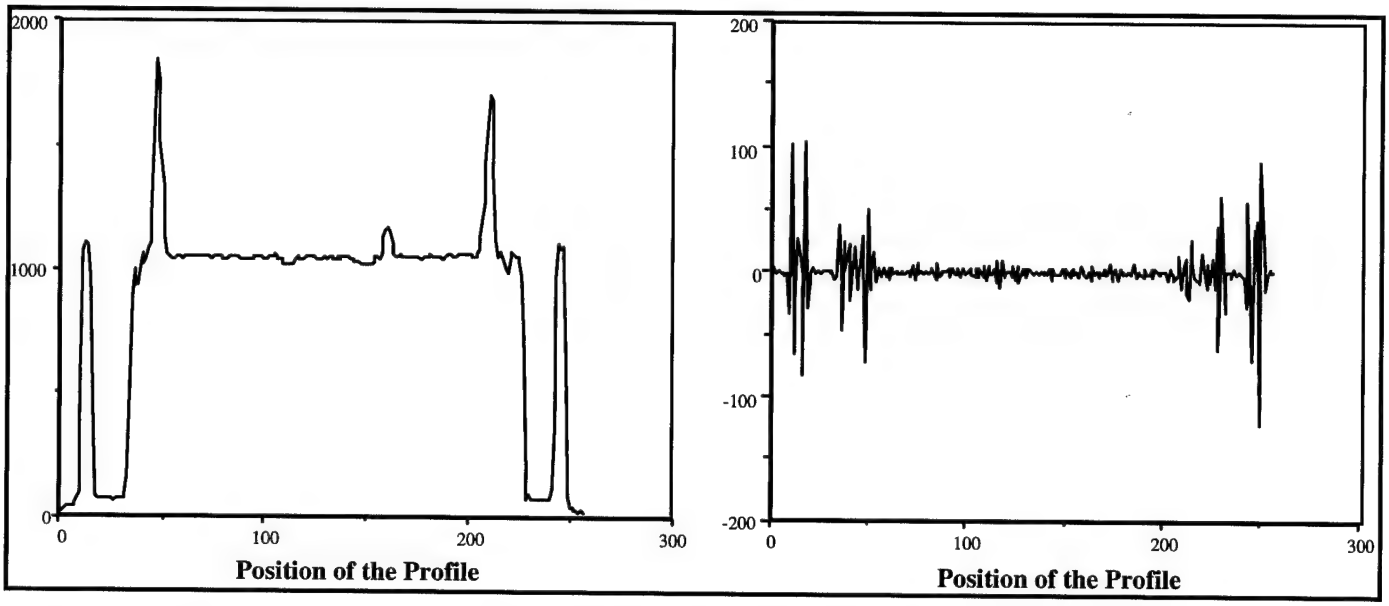

Figure 3. Single level data decomposition through the Daubechies' D8 wavelet filter. The left profile shows the decomposed low pass coefficients. The right profile is the decomposed high pass coefficients with C= 2.115899710319.

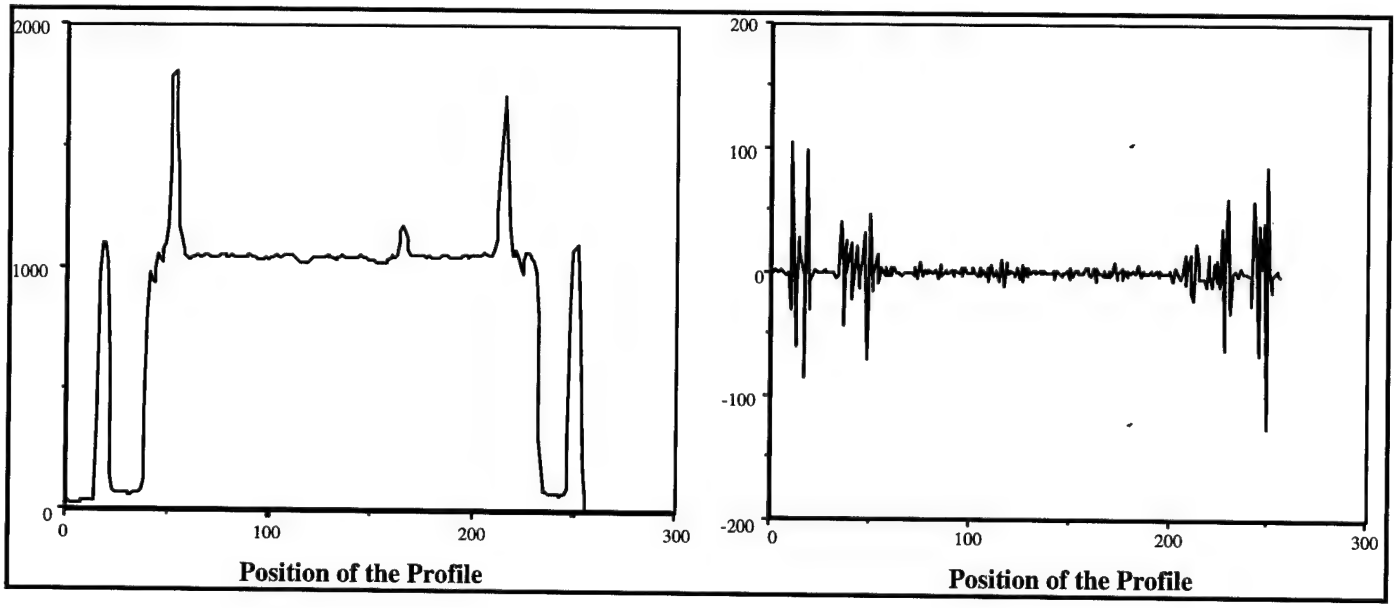

Figure 4. Single level data decomposition through the integer implementation of Daubechies' D8 wavelet. The left profile shows the decomposed low pass coefficients. The right profile is the decomposed high pass coefficients.

2. On Optimzation of Wavelet Kernels for Mammography Image Compression

A neural network based method has been developed to search for optimal wavelet kernels which

can produce the most favorable set of transform coefficients to preserve data accuracy and/or defined image features during the compression. In this study, our technical achievements were: (a) development of a unified method to facilitate multichannel wavelet decomposition; (b) designing a cost (error) function consisting of MSE and imposed entropy reduction function for training the convolution neural network; and (c) converting neural network suggested kernel into a filter constrained by the wavelet requirements.

In all medical image modalities we have tested so far (including mammography, CT, MRI), Daubechies' wavelet (or its nearby wavelets) generally performs better (in most cases slightly better) than other wavelts for image compression using a global measure. With a large quantization factor, Haar's wavelet produces the lowest and highest mean-square-errors for the background and microcalcification profile areas, respectively. However, Daubechies' wavelet produces an opposite result. In addition, we found that the wavelet associated with a low-pass filter, (0.32252136, 0.85258927, 0.38458542, -0.14548269), possesses the highest feature preservation capability in microcalcification peak, contrast, and signal to noise ratio. Through this study, we also found that only Haar's wavelet sometimes produced a dramatic result, usually optimization occurs on a band of wavelets not at a single wavelet [31].

We, therefore, conclude that Daubechies' wavelet (and its nearby wavelets) is generally applicable for image compression. However, Haar's wavelet is suitable for low-noise smooth areas and sharp edges. For a specific image pattern such as microcalcifications on mammograms, one might find a wavelet filter can most preserve the features.

3. Mammography Image Compression Using Wavelet Transform via Integer Computation

We have developed a research software package that is capable of compression any image with a lossless or lossy result controllable by the user. In addition, any wavelet can be approximated by its associated integer implementation in this software as described in section 1.2. This research package allows the user to select desired wavelet. Both lossless and lossy compression were studied on 3 sets of mammograms (4 images per set: MLO and CC views with left and right mammograms as a set) which were digitized with 100 μm and 12 bits per pixel (i.e., ranging 10 Mbytes - 18 Mbytes per image originally). We chose a large, a medium, and a small breasts for each set in our study.

3.1. Lossless Compression Study

We roughly trimmed the air region and the boundary of the films from the originally digitized mammograms. We then performed a lossless compression study using Daubechies' wavelet transform with integer computation method. The results are shown in Table I.

We found that the average compression ratio was about 3.3 based on the trimmed and 12 bit/pixel image. This result was dramatically increased to 11 for medium and large breast images and to 42 for small breast mammograms when using the originally digitized image as bases. This results can further increased by a factor of **1.5** when we mask out the air area in the trimmed images in our computer software. The results of this study will be given in the report of this project next year.

Table I. Compression ratios based on Daubechies' wavelet transform with integer computation

Breast Type	Large Breast		Medium Breast		Small Breast	
View	CC	MLO	CC	MLO	CC	MLO
Orginal Data Size	2,560x3,584x2bytes (18,350,080 bytes)		2,048x2,560x2bytes (10,485,760 bytes)		2,048x2,560x2bytes (10,485,760 bytes)	
Roughly Trimmed Data Size	1,500x2,500x 1.5 bytes (5,625,000)	1,500x2,500x 1.5 bytes (5,625,000)	1,024x2,048x 1.5 bytes (3,145,728)	1,024x2,048x 1.5 bytes (3,145,728)	512x1,024x 1.5 bytes (786,432)	520x1,024x 1.5 bytes (786,432)
Compressed Data Size using the Lossless Method	1,608,316 bytes	1,724,551 bytes	945,675 bytes	993,412 bytes	239,776 bytes	250,343 bytes
Compression Ratio to Trimmed Data	3.50	3.26	3.33	3.17	3.28	3.14
Compression Ratio to original	11.41	10.64	11.09	10.56	43.73	41.89

3.2. Lossy Compression Study

The beauty of the integer wavelet compression method is that the lossless and lossy method can be implemented on the same transform domain. The transformed domain coefficients used in the above lossless compression study were further processed by a quantization procedure (i.e., the values were uniformed divided by a factor in each level of wavelet compartments) followed by a arithmetic coding. The decompressed images were compared to the original images to obtain the normalized mean-square-errors (NMSE). The results are shown in Table II.

Table II. Compression ratios and NMSE values based on Daubechies' wavelet transform with integer computation

Breast Type	Large Breast		Medium Breast		Small Breast	
View	CC	MLO	CC	MLO	CC	MLO
Orginal Data Size	2,560x3,584x2bytes (18,350,080 bytes)		2,048x2,560x2bytes (10,485,760 bytes)		2,048x2,560x2bytes (10,485,760 bytes)	
Roughly Trimmed Data Size	1,500x2,500x 1.5 bytes (5,625,000)	1,500x2,500x 1.5 bytes (5,625,000)	1,024x2,048x 1.5 bytes (3,145,728)	1,024x2,048x 1.5 bytes (3,145,728)	512x1,024x 1.5 bytes (786,432)	520x1,024x 1.5 bytes (786,432)
NMSE (compression ratios)	NMSE=3.3 CR = 2 CR'= 6.52	NMSE=3.3 CR = 2 CR'= 6.52	NMSE=3.5 CR = 2 CR'= 6.67	NMSE=3.4 CR = 2 CR'= 6.67	NMSE=3.5 CR = 2 CR'= 6.67	NMSE=3.4 CR = 2 CR'= 6.67
NMSE (compression ratios)	NMSE=151 CR = 30 CR'= 98	NMSE=148 CR = 30 CR'= 98	NMSE=158 CR = 30 CR'= 100	NMSE=155 CR = 30 CR'= 100	NMSE=159 CR = 30 CR'= 400	NMSE=159 CR = 30 CR'= 400

where CR represents the compression ratio with respect to the trimmed image and CR' stands for the compression ratio with respect to the originally digitized mammograms. All 24 decompressed images do not show observable differences from the original mammograms including microcalcifications in our preliminary viewing on a monitor. Further studies will be performed with CAD-guided lossless compression for the suspicious microcalcifiction and mass areas and the results will be reported next year.

(f) Planning of pilot clinical trial

Dr. Dorfman, Dr. Berbaum, and Dr. Lenth at the University of Iowa have been leading the efforts in planning of the pilot clinical trial and developing methods for statistical analysis of the data to be collected. The data in this research project can be conceptualized in the following way: Patients and readers will be crossed with treatments, and patients will be nested within readers. In brief, readers will participate in both treatments, decision without CADx and decision with CADx. It is assumed that readers and patients are a random sample from their respective populations. The factors are:

Treatments:	2, fixed effect (Control, CADx),
Readers:	9, random effect,
Patients:	5000 (30 cancers expected), random effect nested within readers.

Although our multireader, multipatient algorithms have been used previously to analyze data from experiments with designs similar to that of the proposed studies [32], a major difference is that patients in the current studies are nested within readers rather than crossed over readers. This design is often referred to as a split-plot design in the literature. The linear model for the research is:

$$Pseudovalue = \mu + Reader + Patient(Reader) + Treatment + Treatment \times Reader + Residual$$

where *Patient(Reader)* denotes patients nested within readers, and 'x' denotes interaction. During this last year, we have extended our methodology to this split-plot design. Simulations were performed on both the fully crossed factorial design and the split-plot design. Two papers are currently being prepared for publication that describe the results of these simulations (see Appendix).

Because the prevalence of breast cancer in a screening population is low (about 6 per 1000), the receiver operating characteristic (ROC) rating data will be too sparse for traditional binormal analysis. Sparse data lead to degenerate ROC fits that sometimes cross the chance line. We have developed and evaluated a proper constant-shape bigamma model to handle binormal [33]. Monte Carlo samples were generated both from a standard binormal population model, and from a proper constant-shape bigamma model in a series of Monte Carlo studies. The results confirm Hanley's proposition that the standard binormal model is robust in large samples with no degenerate datasets and Metz's proposition that the standard binormal model is not robust in small samples because of degenerate datasets.

A proper constant-shape bigamma model seems to solve the problem of degeneracy without inappropriate chance line crossings. The bigamma fitting model outperformed the standard binormal fitting model in small samples, and gave similar results in large samples. We are currently implementing a computer program that will permit us to analyze the multireader, multipatient data collected in this research project using these new methods.

(7) Conclusions

We have been developing the CAD workstation and preparing for the pilot clinical study in this year. Except for the slight delay in the GUI development (described below), the project is progressing as planned in the different subprojects. We have migrated to the UNIX operating system. The mass detection program has been improved and compared with our previous results. The wavelet data compression techniques are being investigated, and preliminary planning of the pilot clinical study has been completed.

We have some difficulties in recruiting a computer programmer to develop the GUI. Because of the limited budget for this position, it was very difficult to compete for an experienced programmer due to the high demand for expertise in this area in the industry. The first programmer whom we offered the position accepted another position in a commercial firm after we waited for two months. A second programmer also used our position for a transition time and returned to the industry after about one month on the job. The current programmer initially lacked experience in C++ and GUI. However, he was reliable and hard-working and was able to learn these necessary skills after a relatively short time. He is now well on his way to develop the GUI. This recruitment problem caused some delay in the development of the CAD workstation. We plan to catch up with the scheduled work as soon as possible.

(8) References

1. *National Center for Health Statistics. Vital statistics of the United States, 1987. Vol. 2. Mortality. Part A*, DHHS Publication no. (PHS) 90-1101 (Government Printing Office, Washington, D.C., 1990).
2. C. C. Boring, T. S. Squires, T. Tong and S. Montgomery, "Cancer statistics 1994," CA-A Cancer Journal for Clinicians 44, 7-26 (1994).
3. J. R. Harris, M. E. Lippman, U. Veronesi and W. Willett, "Breast Cancer," N Engl J Med 327, 319-328 (1992).
4. C. R. Smart, R. E. Hendrick, J. H. Rutledge and R. A. Smith, "Benefit of mammography screening in women ages 40 to 49 years: current evidence from randomized controlled trials," Cancer 75, 1619-1626 (1995).
5. C. Byrne, C. R. Smart, C. Cherk and W. H. Hartmann, "Survival advantage differences by age: evaluation of the extended follow-up of the Breast Cancer Detection Demonstration Project," Cancer 74, 301-310 (1994).
6. S. A. Feig and R. E. Hendrick, *Risk, Benefit, and Controversies in Mammographic Screening. In: Syllabus: A categorical Course in Physics Technical Aspects of Breast Imaging*, A. G. Haus and M. J. Yaffe, (Radiological Society of North America, Inc, Oak Brook, IL, 1993).
7. B. N. Curpen, E. A. Sickles, R. A. Sollitto and et. al., "The comparative value of mammographic screening for women 40-49 years old versus women 50-59 years old," AJR 164, 1099-1103 (1995).
8. M. Moskowitz, *Benefit and risk. In: Breast Cancer Detection: Mammography and Other Methods in Breast Imaging*, 2nd ed. Eds. L. W. Bassett and R. H. Gold, (Grune and Stratton, New York, 1987).
9. H. Seidman, S. K. Gelb, E. Silverberg, N. LaVerda and J. A. Lubera, "Survival experience in the Breast Cancer Detection Demonstration Project," CA Cancer J Clin. 37, 258-290 (1987).
10. J. E. Martin, M. Moskowitz and J. R. Milbrath, "Breast cancer missed by mammography," AJR 132, 737-739 (1979).
11. B. J. Hillman, L. L. Fajardo, T. B. Hunter and et. al, "Mammogram interpretation by physician assistants," AJR 149, 907-911 (1987).

12. L. Kalisher, "Factors influencing false negative rates in xeromammography," Radiology 133, 297-301 (1979).
13. L. W. Bassett, D. H. Bunnell, R. Jahanshahi, R. H. Gold, R. D. Arndt and J. Linsman, "Breast cancer detection: one versus two views," Radiology 165, 95-97 (1987).
14. C. J. Baines, A. B. Miller, C. Wall and et. al, "Sensitivity and specificity of first screen mammography in the Canadian National Breast Screening Study: A preliminary report from five centers," Radiology 160, 295-298 (1986).
15. P. J. Haug, I. M. Tocino, P. D. Clayton and T. L. Bair, "Automated management of screening and diagnostic mammography," Radiology 164, 747-752 (1987).
16. M. G. Wallis, M. T. Walsh and J. R. Lee, "A review of false negative mammography in a symptomatic population," Clinical Radiology 44, 13-15 (1991).
17. J. A. Harvey, L. L. Fajardo and C. A. Innis, "Previous mammograms in patients with impalpable breast carcinomas: Retrospective vs blinded interpretation," AJR 161, 1167-1172 (1993).
18. R. E. Bird, T. W. Wallace and B. C. Yankaskas, "Analysis of cancers missed at screening mammography," Radiology 184, 613-617 (1992).
19. C. E. Metz and S. Shen, "Gains in diagnostic accuracy from replicated readings of diagnostic images: prediction and assessment in terms of ROC analysis," Med Decis Making 12, 60-75 (1992).
20. E. L. Thurfjell, K. A. Lernevall and A. A. S. Taube, "Benefit of independent double reading in a population-based mammography screening program," Radiology 191, 241-244 (1994).
21. H. P. Chan, K. Doi, C. J. Vyborny, R. A. Schmidt, C. E. Metz, K. L. Lam, T. Ogura, Y. Wu and H. MacMahon, "Improvement in radiologists' detection of clustered microcalcifications on mammograms. The potential of computer-aided diagnosis," Invest Radiol 25, 1102-1110 (1990).
22. W. P. Kegelmeyer, J. M. Pruneda, P. D. Bourland, A. Hillis, M. W. Riggs and M. L. Nipper, "Computer-aided mammographic screening for spiculated lesions," Radiology 191, 331-337 (1994).
23. L. Tabar and P. B. Dean, *Teaching Atlas of Mammography*, (Thieme, New York, 1985).
24. F. Shtern, C. Stelling, B. Goldberg and R. Hawkins, "Novel technologies in breast imaging: National Cancer Institute perspective," Society of Breast Imaging, Orlando, Florida, 153-156 (1995).
25. A. N. Akansu and R. A. Haddad, *Multiresolution Signal Decomposition*, (Academic Press, San Diego, CA, 1992).
26. V. K. Heer and H.-E. Reinfelder, "A comparision of reversible methods for data compression," Proc. SPIE 1233, 354-365 (1990).
27. I. Daubechies, "Orthonormal based of compactly supported wavelets," Comm. on Pure and Appl. Math XLI, 909-996 (1988).
28. S. C. Lo, J. Xuan, H. Li, Y. Wang, M. T. Freedman and S. K. Mun, "Dyadic decomposition: A unified perspective on predictive, subband, and wavelet transforms," Proc. SPIE 3031, 286-301 (1997).
29. J. Shapiro, "An embedded hierarchical image coder using zerotrees of wavelet coefficients," Proc. IEEE Data Compression Conf '93 214-223 (1993).
30. A. Said and W. A. Pearlman, "Reversible image compression via multiresolution representation and predictive coding," Proc. SPIE 2094, 664-674 (1993).
31. S. C. Lo, H. Li and Y. Wang, "Optimization of wavelet decomposition through neural network search," WCNN, INNS Press 278-283 (1996).
32. D. D. Dorfman, K. S. Berbaun and C. E. Metz, "ROC rating analysis: Generalization to the population of readers and cases with the jackknife method," Invest. Radiol. 27, 723-731 (1992).

33. D. D. Dorfman, K. S. Berbaum, C. E. Metz, R. V. Lenth, J. A. Hanley and H. Abu-Dagga, "Proper Receiver Operating Characteristic analysis: The bigamma model," Academic Radiology 4, 138-149 (1997).

(9) Appendix

Publications (University of Michigan)

1. Chan HP, Sahiner B, Lam KL, Petrick N, Helvie MA, Goodsitt MM, Adler DD. Computerized analysis of mammographic microcalcifications in morphological and texture feature spaces. Medical Physics 1997 (Submitted).

2. Sahiner B, Chan HP, Petrick N, Helvie MA, Goodsitt MM. Development of a high-sensitivity classifier for computer-aided diagnosis: Application to classification of malignant and benign masses. Physics in Medicine and Biology 1997 (Submitted).

3. Petrick N, Chan HP, Sahiner B, Helvie MA, Adler DD, Goodsitt MM. Computer Vision Techniques for Detection of Mammographic Masses. Scientific Exhibit at the 82nd Scientific Assembly and Annual Meeting of the Radiological Society of North America, Dec 1- 6, 1996, Chicago, Illinois. Radiology 1996; 201(P): 524.

4. Chan HP, Sahiner B, Wagner RF, Petrick N. Classifier design for computer-aided diagnosis in mammography: Effects of finite sample size. CAD in Mammography Symposium at the 39th Annual Meeting of the American Association of Physicists in Medicine. Milwaukee, Wisconsin, July 27-31, 1997. Medical Physics 1997; 24: 1034.

5. Sahiner B, Chan HP, Petrick N, Gopal S, Goodsitt MM. Neural network design for optimization of the partial area under the receiver operating characteristic curve. Proc. of the 1997 International Conference on Neural Networks (ICNN'97) 1997; 4: 2468-2471.

6. Gopal S, Sahiner B, Chan HP, Petrick N. Neural network based segmentation using *a priori* image models. Proc. of the 1997 International Conference on Neural Networks (ICNN'97) 1997; 4: 2455-2459.

7. Petrick N, Chan HP, Sahiner B, Helvie MA, Gopal S, Goodsitt MM. Computer-Aided Detection of Breast Masses: Evaluation of a Fuzzy Morphological Classifier. Accepted for presentation at the 83rd Scientific Assembly and Annual Meeting of the Radiological Society of North America, Nov 30-Dec 5, 1997, Chicago, Illinois.

8. Gopal S, Sahiner B, Petrick N, Chan HP, Helvie MA, Wilson TE. Evaluation of automated methods for the segmentation of mass boundaries on mammograms for computer aided diagnosis (CAD) applications. Accepted for presentation at the 83rd Scientific Assembly and Annual Meeting of the Radiological Society of North America, Nov 30-Dec 5, 1997, Chicago, Illinois.

9. Chan HP, Sahiner B, Helvie MA, Paramugul C, Newman JS, Gopal S, Petrick N, Adler DD, Roubidoux MA, Wilson TE. Effects of computer-aided diagnosis (CAD) on radiologists' classification of malignant and benign masses on mammograms: an ROC study. Accepted for presentation at the 83rd Scientific Assembly and Annual Meeting of the Radiological Society of North America, Nov 30-Dec 5, 1997, Chicago, Illinois.

10. Chan HP, Petrick N, Gopal S, Wilson TE, Roubidoux MA, Adler DD, Sahiner B, Helvie MA, Paramugul C, Newman JS. Observer performance studies of the effects of computer-aided diagnosis (CAD) on radiologists' classification of malignant and benign masses on mammograms. Accepted for Scientific Exhibit at the 83rd Scientific Assembly and Annual Meeting of the Radiological Society of North America, Nov 30-Dec 5, 1997, Chicago, Illinois.

Publications (Georgetown University)

1. Lo, S.C., Li, H., Wang, Y., Freedman, M.T., and Mun, S.K., "On Optimization of Orthonormal Wavelet Decomposition: Data Accuracy, Feature Preservation, and Compression," SPIE Proceedings, Medical Imaging on Image Display, 1996, Vol. 2707, pp. 201-214.

2. Lo, S.C., Li, H., Wang, Y., "Optimization of Wavelet Decomposition through Neural Network Search," WCNN, INNS Press, 1996, pp. 278 - 843.

3. Lo, S.C., Xuan, J., Li, H., Wang, Y., Freedman, M.T., and Mun, S.K., "Dyadic Decomposition: A Unified Perspective on Predictive, Subband, and Wavelet Transforms", SPIE Proceedings on Medical Imaging, 1997, vol. 3031, (in press).

4. Li, H., Lo, S.C., Wang, Y., Freedman, M.T., and Mun, S.K., "Mammographic Mass Detection by Stochastic Modeling and a Mutli-Modular Neural Network, SPIE Proceedings on Medical Imaging 1997, vol. 3034, (in press).

Publications (University of Iowa)

1. Dorfman DD, Berbaum KS, Lenth RV, Chen Y-F. Monte Carlo validation of a multireader method for analyzing receiver operating characteristic discrete rating data: Factorial experimental design. In preparation, 1997.

2. Lenth RV, Dorfman DD, Berbaum KS, Chen Y-F. Monte Carlo validation of a multireader method for analyzing receiver operating characteristic discrete rating data: Split-plot experimental design. In preparation, 1997.